(2)

ポジトロンエミッショントモグラフィを用いた脳賦活検査の基礎的研究

定藤　規弘

Noninvasive Measurement of Regional Cerebral Blood Flow Change with $H_2{}^{15}O$ and Positron Emission Tomography Using a Mechanical Injector and a Standard Arterial Input Function

Norihiro Sadato, MD ; Yoshiharu Yonekura, MD†; Michio Senda, MD *; Yasuhiro Magata, PhD; Yasushi Iwasaki, MD; Naoki Matoba, MD; Tatsuro Tsuchida, MD; Nagara Tamaki, MD ; Hidenao Fukuyama, MD¶; Hiroshi Shibasaki, MD†; Junji Konishi, MD

Departments of Nuclear Medicine, †Brain Pathophysiology, and ¶Neurology, Kyoto University Faculty of Medicine, Kyoto, and *Tokyo Metropolitan Institute of Gerontology, Tokyo, JAPAN

For correspondence and reprint requests:

Norihiro Sadato, MD

Department of Nuclear Medicine, Kyoto University

Faculty of Medicine

54 Kawahara cho, Shogoin, Sakyo ku, Kyoto,

606-01, Japan

Telephone: 81-75-751-3419

FAX: 81-75-751-3217

Running head: Measurement of rCBF with $H_2{}^{15}O$ and PET

Abstract

To estimate changes in regional cerebral blood flow (rCBF) without arterial sampling in the study of functional-anatomical correlations in the human brain, using ^{15}O-labeled water and PET, a standard arterial input function was generated from the input function in 10 normal volunteers with dose calibration and peak time normalization. The speed and volume of injection were precisely controlled with a mechanical injector. After global normalization of each tissue activity image, the standard arterial input function was applied to obtain estimated CBF images. Relative changes in estimated rCBF to whole brain mean CBF(ΔFest) and those in regional tissue activity (ΔC) were compared with true relative rCBF changes (ΔF) in 40 pairs of images obtained from 6 normal volunteers. ΔFest correlated well with ΔF, whereas ΔC consistently underestimated ΔF. This noninvasive method simplifies the activation studies and provides the accurate estimation of relative flow changes.

Key words: positron emission tomography, cerebral blood flow, activation study, methodology

Introduction

Positron emission tomographic (PET) measurements of regional cerebral blood flow (rCBF) with intravenously administered ^{15}O-labeled water are well suited to the study of functional-anatomical correlations within the human brain [1,2]. Quantification of the change in rCBF from an initial resting state is important for the expression of regional neuronal activation [3]. The measurement of rCBF with PET usually requires serial arterial blood sampling to accurately determine the arterial input function of the tracer. For functional brain mapping, however, the calculation of absolute blood flow values may not be required. Instead, relative changes in rCBF can provide substantial information about the cerebral responses to neurobehavioral tasks [3]. Therefore, the measurement of relative changes in cerebral blood flow without arterial sampling would be preferable.

For wide clinical application, noninvasive and simplified techniques for quantifying relative changes in rCBF have been sought by other investigators [1,3].The near-linear relation between radiotracer concentration and rCBF implies that the distribution of radiotracer concentration closely approximates the rCBF distribution [2]. However, relative changes in simple radiotracer concentration underestimates relative rCBF changes in the gray matter, which is the main concern of activation studies [2,3]. Fox et al [1] proposed a method for correcting the underestimation of rCBF for a region of interest, but not on a pixel-by-pixel basis. In the present paper, we show that correction for the nonlinear relationship between radiotracer concentration and rCBF is essential for quantification of relative changes in CBF. We present a method that can account for this nonlinearlity in estimating relative CBF changes over the whole brain without arterial sampling. The technique utilizes a standard arterial input function and a reference table for the calculation of blood flow [4].

Theory

CBF Measurement

Measurement of CBF was performed by an adaptation of Kety's diffusible autoradiographic method [4-6]. The regional change in cerebral radiotracer concentration is described as

$$\frac{dC_T(t)}{dt} = EFC_a(t) - EF\frac{C_T(t)}{\mu} - \lambda C_T(t) \qquad (1)$$

where $C_T(t)$ is the tissue concentration of $H_2{}^{15}O$ measured by PET, Ca(t) is the arterial concentration of $H_2{}^{15}O$ measured by blood sampling, F is the regional blood flow, μ is the partition coefficient of water between brain and blood, and λ is the physical decay constant of ^{15}O. E is the extraction fraction of the tracer between capillaries and tissues [5, 6].

PET value C obtained by the scan from $t = t_1$ to $t = t_2$ is

$$C = \frac{1}{t_2 - t_1}\int_{t_1}^{t_2} F\, Ca(t) * \exp[-(F/\mu + \lambda)]\, dt \qquad (2)$$

where * indicates convolution. Here, we assumed the extraction fraction was equal to unity [5]. The "look-up" reference table function F = G(C) was generated to relate F to C [4], and applied to the PET images of radioactivity pixel-by-pixel to calculate rCBF.

Measurement of Relative Change in rCBF

Global normalization

In an activation study, the primary concern is to locate and quantitate rCBF changes induced by the activation paradigm [7], because global (whole-brain) CBF is not significantly affected by passive sensory stimulation [8, 9] or motor tasks [10, 11]. The fluctuation of global CBF (gCBF) between successive scans in the current study (the mean within-subject coefficient of variation was 5.1%) was similar to that observed in previous studies [8-11]. The fluctuation could be caused by technical problems such as insufficient temporal sampling of arterial blood, or by failure to correct the delay and dispersion of the input function [6,12,13]. Physiological factors, such as the variation of P_aCO_2, might also have contributed [11]. The effect of fluctuation of gCBF was effectively abolished by multiplying each pixel by a correction factor calculated as the scan gCBF divided by the true mean gCBF [1,7-10]. This method, global normalization, has been proved to allow quantitative comparison of the relative regional increase in radiotracer concentration and blood flow induced by selective stimulation [1]. This process assumes that scan-to-scan fluctuation equally affects every pixel used for calculation of gCBF and that the contribution of the activated region to the variation in gCBF is small relative to that of gCBF [9].

Relative change in rCBF

In the neurobehavioral task batteries, we consider state 1 (control) and state 2 (activation) of the same subject. The reference tables of each state are $G_1(C)$ and $G_2(C)$, respectively. The simple radiotracer concentrations at one pixel are C_1 and C_2 .The corresponding rCBFs F_1 and F_2 are $F_1 = G_1(C_1)$, $F_2 = G_2(C_2)$. The global means of CBF in each state are F_{1g} and F_{2g} . Using F_{1g} and F_{2g} , F_1 and F_2 are expressed as:

$$F_1 = yF_{1g}$$
$$F_2 = (y+\Delta y)F_{2g} \qquad (3)$$

where variable y represents the CBF of state 1 relative to F_{1g}, and $y+\Delta y$ of state 2. The relative change in CBF, ΔF, is expressed with radiotracer concentrations and reference table functions of each state as follows:

$$\Delta F = \frac{\Delta y}{y} = \frac{gF_2}{F_1} - 1 = \frac{gG_2(C_2)}{G_1(C_1)} - 1 \qquad \text{where } g = \frac{F_{1g}}{F_{2g}} \qquad (4)$$

Similarly, C_1 and C_2 can also be expressed as:

$$C_1 = xC_{1g}$$
$$C_2 = (x + \Delta x)C_{2g} \qquad (5)$$

where variable x represents the radiotracer concentration relative to the global concentration in state 1. With Equation 5, Equation 4 is expressed as:

$$\Delta F = \frac{gG_2((x + \Delta x)C_{2g})}{G_1(xC_{1g})} - 1 \qquad (6)$$

A fractional increase propagation function H(C) is defined as

$$H(C) = \frac{dG/G}{dC/C} \qquad (7)$$

which is the ratio of the fractional increase in the CBF to the fractional increase in the measured radiotracer concentration.

For a small ΔC,

$$G(C + \Delta C) = G(C) + G(C)\frac{\Delta C}{C}H(C) = G(C)(1 + \frac{\Delta C}{C}H(C)) \qquad (8)$$

Therefore, if Δx is small, this relationship may be applied to the numerator of Equation 6:

$$G_2((x+\Delta x)\, C_{2g}) = G_2(xC_{2g} + \Delta(xC_{2g}))$$

$$= G_2(x\, C_{2g}) + G_2(x\, C_{2g})\, \frac{\Delta(xC_{2g})}{xC_{2g}}\, H_2(x\, C_{2g}) \qquad (9)$$

where H_2 is the fractional increase function at state 2.

Using this expression for the numerator of Equation 6, ΔF can be expressed with a fractional increase propagation function H_2 as

$$\Delta F = \frac{gG_2(x\, C_{2g})}{G_1(xC_{1g})}\,(1 + \frac{\Delta x}{x} H_2(xC_{2g})) - 1 \qquad (10)$$

noting that

$$\frac{\Delta(xC_{2g})}{xC_{2g}} = \frac{\Delta x}{x}$$

since C_{2g} is constant. Moreover, C_{1g} and C_{2g} are considered to be constant, $G_1(xC_{1g})$, $G_2(xC_{2g})$, and $H_2(xC_{2g})$ are the functions of x. Thus

$G_1(xC_{1g}) = \hat{G}_1(x)$, $G_2(xC_{2g}) = \hat{G}_2(x)$:systematic normalized reference table function

$H_2(xC_{2g}) = \hat{H}_2(x)$:normalized increase propagation function.

Using this notation, ΔF is expressed as

$$\Delta F = \frac{g\hat{G}_2(x)}{\hat{G}_1(x)}\,(1 + \frac{\Delta x}{x}\hat{H}_2(x)) - 1$$

$$= J(x)\,(1 + \frac{\Delta x}{x}\hat{H}_2(x)) - 1 \qquad (11)$$

where

$$J(x) = \frac{g\hat{G}_2(x)}{\hat{G}_1(x)} = \frac{\frac{\hat{G}_2(x)}{F_{2g}}}{\frac{\hat{G}_1(x)}{F_{1g}}} \qquad (12)$$

J(x) is the ratio of the relative blood flow of consecutive scans to the corresponding relative concentration of radiotracer (x) . If G_1 and G_2 are linear,

$\frac{\hat{G}_1(x)}{F_{1g}} = \frac{\hat{G}_2(x)}{F_{2g}} = x$

then J(x) = 1. If, in addition, $\hat{H}_2(x) = 1$, then $\Delta F = \frac{\Delta x}{x}$. This is not the case, however, as washout of the radiotracer causes nonlinearity between C and F. When the relative change in CBF, ΔF, is estimated by the relative change in radiotracer concentration, $\Delta C = \frac{\Delta x}{x}$, the systematic error is

$$\Delta C - \Delta F = \frac{\Delta x}{x}(1 - \hat{H}_2(x)J(x)) + (1 - J(x)) \qquad (13)$$

In this paper, we propose a standard reference table function Gs(C), which was derived from the standard arterial input function obtained from measured arterial curves in 10 normal subjects. In this method, radiotracer concentration images are globally normalized to Cs, which is the standard global mean of radiotracer concentration determined independently. Gs(C) was then applied to the normalized images. Estimated relative change in rCBF is then expressed as:

$$\Delta F_{est} = \frac{G_S(\alpha_2 C_2) - G_S(\alpha_1 C_1)}{G_S(\alpha_1 C_1)} \quad \text{where} \quad \alpha_1 = \frac{C_S}{C_{1g}} \quad \alpha_2 = \frac{C_S}{C_{2g}} \qquad (14)$$

Using the definitions of C_1 and C_2 given in Equation 5, Equation 14 may be expanded as:

$$\Delta F_{est} = \frac{G_S((x + \Delta x)C_S) - G_S(xC_S)}{G_S(xC_S)} = \frac{G_S((x + \Delta x)C_S)}{G_S(xC_S)} - 1 \qquad (15)$$

If Δx is relatively small, $G_S((x + \Delta x)C_S)$ may be approximated in terms $H_S(xC_S)$ using a derivation and notation similar to those used in simplifying $G_2((x + \Delta x)C_{2g})$ in Equations 6-8:

$$\Delta F_{est} = (1 + \frac{\Delta x}{x} H_S(xC_S)) - 1 = \frac{\Delta x}{x}\hat{H}_S(x) \qquad (16)$$

The systematic error in estimating ΔF by ΔFest is expressed as follows using Equation 11:

$$\Delta F_{est} - \Delta F = \frac{\Delta x}{x} (\hat{H}_S(x) - \hat{H}_2(x)J(x)) + (1 - J(x)) \qquad (17)$$

This error is small when $\hat{H}_2(x)$ is well approximated by $\hat{H}_S(x)$ and when J(x) is close to unity. Since delay and dispersion of the arterial input function affect the shape of the reference table [5], strict control of the speed and volume of injection was attempted to increase the reproducibility of the input functions. In that situation, J(x) would be near unity, because relative blood flow of consecutive scans corresponding to the same relative concentration of radiotracer (x) is expected to be the same. In addition, variability in $\hat{H}_2(x)$ would be small, because the shapes of the reference tables are probably similar, even interindividually. A standard input function can be generated by averaging the input functions after dose calibration and peak time normalization. Using the standard input function, a standard reference table $\hat{G}_S(x)$ can be calculated, where C_S is selected to fit $\hat{H}_S(x)$ to the mean $\hat{H}_2(x)$ at each x. To quantitate the relative change in rCBF noninvasively, tissue activity images are globally normalized with $\alpha = Cs/Cg$, then the standard reference table $F = Gs(C)$ is applied to generate normalized CBF images of states 1 and 2. The activation-induced change in rCBF is then obtained by pixel-by-pixel subtraction of the normalized CBF images of state 1(control) from that of state 2(activated).

Materials and Methods

Tomograph Characteristics

The PCT-3600W system (Hitachi Medical Co., Japan) was employed for PET scanning [14]. This system simultaneously acquires 15 slices with a center-to-center interslice distance of 7 mm. All scans were performed at a resolution of 9 mm full width at half maximum (FWHM) in the transaxial direction and 6.5 mm in the axial direction. Field of view and pixel size of the reconstructed images were 256 mm and 2 mm, respectively. Tomographic transmission data,using a standard Ge-68/Ga-68 plate source, was obtained before all emission measurements.

Subject Preparation

Ten normal volunteers (all men, aged 20-25 years) were studied. Six of them participated in an activation study involving a finger-movement paradigm and PET. The remaining four participated in other activation studies, and their arterial radiotracer activity curves were used only to obtain the standard arterial input function. Written informed consent was obtained from each subject using forms and procedures approved by the Ethical Committee of Kyoto University Faculty of Medicine.

A catheter was placed in the cubital vein of the subject's right arm and the brachial artery of the left arm. The subject lay in a resting state, with eyes closed, and the room was quiet and dimly lit. No attempt was made to control the subject's thought content. During scanning, the head was immobilized with an individually molded head-holder.

Behavioral States

Two scans were acquired while the subjects were at rest; no stimulation was given and no task was performed (state 1, control). Two to four scans were performed while the subjects moved the fingers in the right hand (state 2, activation). A total of 31 measurements were performed, including 12 control states and 19 activation states.

Tracer Techniques

Scan acquisition of 90 seconds was initiated at the start of tracer injection. Data were collected on six consecutive frames of 15 seconds each. The sinograms were added to make one static PET image.

$H_2{}^{15}O$ was injected into the right cubital vein (6 ml in 15 seconds) with an automatic injector. Arterial blood samples were obtained manually from the left brachial artery every 3 to 5 seconds after the radiotracer was injected until scanning was completed to obtain the arterial input curve. The volume and activity of residual radiotracer in the syringe were measured and corrected for decay to obtain the injected dose.

Data Analysis

Reference table

The reference table function G(C) was calculated from Equation 2, using the measured arterial input function. The arterial activity curve Ca(t) was determined by multiple blood samplings starting from $t = 0$ with linear interpolation between measured points. For each CBF value from F = 0 to 130 ml/min/100 g in steps of 0.2 flow units, the average tissue activity, C, was calculated from Equation 2. The relation between blood flow and tissue radiotracer concentration (reference table) was approximated by a 4th order polynomial equation for each scan. J(x) and H(x) were obtained from G(C), global CBF, and global radiotracer concentration. Global radiotracer concentration (Cg) and global CBF (Fg) were determined for each scan. First, a template for each subject was obtained from the tissue activity image of the initial resting state. The template consisted of all pixels having 30% or more of the maximum activity in the 15 slices. This 30% cut-off method can effectively eliminate nonbrain structures, such as the cranium and

ventricles. This was confirmed by direct comparison of the template and the magnetic resonance images of the brain in each subject. Fg and Cg were then calculated for each scan by averaging the values of all pixels in the template.

Standardization of arterial input function

Arterial input function data were obtained from all 10 subjects, including the six involved in the finger-movement paradigm. Two series of arterial samplings were performed while subjects were in a resting state, during which no stimulation was given and no task was performed.

The arterial input function was normalized to correspond to an injected dose of 10 mCi of $H_2{}^{15}O$. Each dose-normalized arterial input function was shifted to the mean peak time. These shifted curves were averaged to obtain the standard input function. A standard reference table was calculated as, described earlier.

Determination of Cs and Gs(Cs)

While $H_S(C)$ is determined by $G_S(C)$, $\hat{H}_S(x)$ depends on Cs. For accurate estimation of the mean $\hat{H}(x)$ by $\hat{H}_S(x)$ in a wide range of x, Cs was chosen to minimize the mean absolute error in the range of x (0 -1.5). The standard global mean of blood flow (Fs) was defined as Fs = Gs(Cs).

Calculation of relative change in rCBF with standard reference table(ΔFest)

To determine the systematic errors in relative changes of rCBF (ΔF) by the relative changes in radiotracer concentration (ΔC) and by the relative changes

estimated with the standard reference table method (ΔFest), ΔC, ΔF, and ΔFest were calculated using the following equations:

$$\Delta C = \frac{\alpha_2 C_2 - \alpha_1 C_1}{\alpha_1 C_1}$$

$$\Delta F = \frac{\beta_2 G_2(C_2) - \beta_2 G_1(C_1)}{\beta_2 G_1(C_1)}$$

$$\Delta Fest = \frac{G_S(\alpha_2 C_2) - G_S(\alpha_1 C_1)}{G_S(\alpha_1 C_1)}$$

where $\alpha_1 = C_s/C_{1g}$, $\alpha_2 = C_s/C_{2g}$.

Since measured CBF images were globally normalized to 50 ml/min/100 g,

$\beta_1 = 50/F_{1g}$, $\beta_2 = 50/F_{2g}$.

Results

Mean value of J(x), the ratio of relative CBF to the corresponding relative tissue radiotracer activity x, over-all within-subject control-activation study pairs, was distributed in the range of 0.992 to 1.006 with a coefficient of variation less than 1.678 % over a range of x from 0.1 to 1.5. Figure 1 and Table 1 show the reproducibility of $\widehat{H}(x)$ over a range of x from 0.1 to 1.5. The increase propagation factor at the global mean of radiotracer concentration ($\widehat{H}(1)$) was 1.21 $\pm$ 0.04 (mean $\pm$ SD) .

The standard arterial input function obtained from the 10 subjects is shown in Figure 2. Peak time of this curve was 36 seconds, peak value 3133 nCi/ml, and delay time 20 seconds.

The standard reference table was calculated from the standard arterial input function and Equation 2, and was fit to a 4th order polynomial,

$$G_S(C) = 3.1454 \times 10^{-2} + 0.17082C + 1.7565 \times 10^{-4}C^2 - 1.5639 \times 10^{-7}C^3 + 5.2443 \times 10^{-10}C^4$$

Maximum and mean error in terms of absolute value in the range of Gs (0 - 130 ml/min/100 g) were 0.26 and 0.09 ml/min/100 g, respectively.

$\widehat{H}_s(x)$ was well fit to the mean of $\widehat{H}(x)$ over a range of x from 0.1 to 1.5 when Cs was 237 nCi/ml (Table 1). The standard global mean of CBF, Fs = Gs(Cs) , was 50 ml/min/100 g, which was almost equal to the mean of gCBF calculated with the measured input function (49.5 $\pm$ 7.9, mean $\pm$ S.D.).

Table 2 shows a systematic underestimation of ΔF by ΔC ($p < 0.01$; ANOVA), as reported by Fox et al [1]. This underestimation was observed in the low, middle, and high flow range(F = 30, 50, 70 ml/min/100 g). The underestimation increased as ΔF and F increased. The ΔFest was an accurate estimate of the true ΔF without the systematic underestimation found with ΔC over a range of ΔF from 0 to 40% at variable flow values (F = 30, 50, 70 ml/min/100 g) (Tables 2 and 3).

Discussion

The present method permits accurate estimation of changes in rCBF with $H_2{}^{15}O$ and PET noninvasively using a standard input function. Fox et al [2] and Herscovitch et al [12] reported that the nearly linear relation between C (regional tissue radioactivity) and F (regional CBF) inherent in the PET/autoradiographic model indicates that changes in rCBF will be closely approximated by changes in C. Fox et al [1] expressed the relation between C and F as:

$$F = a(C)^2 + b(C)$$

where a and b are constants determined for each scan using a reduced polynomial regression. They further showed that when changes are expressed as fractional changes from initial control measurement, relative changes in rCBF(ΔF) can be calculated with those in tissue activity (ΔC) with the equation

$$\Delta F = \Delta C + \Delta C(\Delta C + 1)\,\alpha$$

where

$$\alpha = 1 + b\left(\frac{b - \sqrt{b^2 + 4af_c}}{2af_c}\right),$$

and f_C is the rCBF within the region of interest (ROI) during the control state.

Therefore, α should depend on the scan, the subject, and the flow values in each ROI. Fox et al [1] showed that α is relatively constant across the subjects in the ROI taken in the striate cortex. For estimation of relative blood flow change, they used the mean value of α ($\overline{\alpha}$) from the initial control scans from 8 normal volunteers, and estimated flow change as:

$$\Delta Fest = \Delta C + \Delta C(\Delta C + 1)\,\overline{\alpha}.$$

Since $\overline{\alpha}$ is still flow-dependent, to estimate the CBF changes in the ROI other than striate cortex, one should know the value of fc, regional CBF in the control state [1]. This process makes it impossible to apply their method on a pixel-by-pixel basis to the whole image. The estimation of relative change of rCBF must be restricted to the specific ROI whose resting blood flow is already known.

In this study, we deduced a more general expression of the relation between ΔF and ΔC, Equation 10, without any need for knowing fc:

$$\Delta F = J(x)\,(1 + \Delta C\,\hat{H}_2(x)) - 1 \quad .$$

As our results show, J(x) is quite close to unity. Since unity of J(x) means that in each individual the same relative radiotracer concentration will accompany the same relative CBF values in the consecutive sessions, this result is reasonable. This is probably because intra-subject reproducibility of shape and delay of input functions between control and activation states is high, and in turn, the normalized reference tables $\hat{G}_1(x)$ and $\hat{G}_2(x)$ are similar in each individual. The similarity could be due to the strict control of speed and volume of injection provided by a mechanical injector. In this case, we can simplify Equation 10 as:

$$\Delta F = \hat{H}_2(x)\,\Delta C \qquad (18).$$

Comparing Equation 18 with Equation 16 shows that the utility of the proposed method for estimating ΔFest depends on the accuracy with which $\hat{H}_2(x)$ is estimated when arterial samples are not obtained. As shown in Table 1, the coefficient of variation of $\hat{H}_2(x)$ among subjects is small over a wide range of relative radiotracer concentration(0.1-1.5). Therefore, to quantify relative CBF changes, the nonlinear relationship between C and F can be systematically corrected with a standard reference table. This is in contrast to the fact that absolute quantification of CBF and CBF changes need individual arterial input function, because they are quite sensitive to the shape of the input function [5, 13,15].

To substitute $\hat{H}_2(x)$ with $\hat{H}_S(x)$, we planned to obtain the standard arterial input function and the standard reference table $G_S(C)$, which in turn can generate $\hat{H}s(x)$, which was best fit to the mean $\hat{H}(x)$ by selecting proper C_S. If the method of radiotracer injection is constant across the subjects, the delay and the shape of the arterial input function are expected to be similar, even interindividually for normal subjects. Mazziotta et al [3] reported that by examining the arterial blood time-activity curves in over 10 normal subjects after a bolus injection of $H_2{}^{15}O$, both the shape and the tracer appearance time were found to be very similar[3]. In our study, however, the tracer appearance time varied from subject to subject. On the basis of these findings, we obtained a standard arterial input function from normal volunteers using mechanical injection with exact dose measurement. We averaged arterial input functions after dose calibration and peak time normalization, to preserve the shape of the input function.

As C_S was selected just to fit $\hat{H}_s(x)$ to the mean value of $\hat{H}(x)$, $F_S = G(C_S)$ is not necessarily the global mean of each scan calculated with the standard reference table. If intersubject averaging is attempted, global normalization of each scan calculated with a standard reference table should be performed. This will not affect our results, as

global normalization is a linear transformation. Similarly, $G_s(\alpha_1 C_1)$ is not necessarily equal to $\beta_1 G_1(C_1)$. We used the normalized CBF value calculated from the measured arterial input of state 1($\beta_1 G_1(C_1)$) for comparison of systematic error of ΔF by ΔFest at different blood flows (Table 2).

At $\Delta F = 0.3$, there was no systematic error for estimation of ΔF by ΔFest at a wide range of CBF values (Table 2). As relative changes in regional blood flow of 0.3 to 0.5 are not readily achieved [1], most ΔF measurements are less subject to error.

The nonlinear count-flow relationship increases as scan time is prolonged, because of increased tracer washout. This has a particularly greater effect on the higher flow region [3]. To avoid underestimation of relative flow changes by the tissue activity changes in the gray matter, scanning for less than 60 seconds from the arrival of the tracer to the brain was recommended [2,3], although even with 40-second scanning, ΔC underestimated ΔF [1]. In this study, underestimation of ΔF by ΔC was greater than that reported by Fox et al [1], because our protocol used a longer scanning time.

Although a shorter scanning time is better to detect relative flow change, longer imaging time might be favored as a compromise between statistical noise and detection sensitivity [3]. If the injected dose is reduced or the detection sensitivity of the tomograph is lower, application of a standard reference table serves to preserve detectability of flow changes. Quantification of relative flow changes is particularly important when the images are analyzed with ROIs because of partial volume effect.

Correction of delay and dispersion of the arterial input function is essential for accurate estimation of CBF [13]. In this study, however, the correction was not performed for the following reasons. First, we adopted manual arterial sampling, in which external delay and dispersion were negligible. Second, it is impossible to measure the internal delay time and dispersion constant with the single-frame autoradiographic method. With the dynamic method, mean internal dispersion time is

estimated at 5 seconds if blood is sampled at the radial artery [13], and differences of arrival time (" head-to-hand " time lag) are 3 seconds [16]. However, the correction is not practical, as internal delay and dispersion depend on the site of arterial sampling (radial artery vs brachial artery) and on the location of the brain region [17]. Finally, the failure to correct the delay and dispersion may be acceptable because of the relatively long scan acquisition time used [13].

Incomplete extraction of water is another cause of the nonlinear count-flow relationship [6,18,19]. Unfortunately, the different values for the permeability-surface area product of water obtained under varying conditions indicated its variability and the difficulty in choosing a value for general use [6,18,19]. Nevertheless, an extraction correction may still be beneficial for an activation study to enhance the flow changes in the higher flow region, which is our primary concern. The relationship between values for CBF measured by PET (F) and the extraction-fraction-corrected CBF (Fcorr) is known as:

$$Fcorr = F/[1-\exp(-PS/Fcorr)] \qquad (19)$$

where PS is the permeability-surface area product of water [6]. Thus, there is no way to algebraically solve for Fcorr in terms of F. However, Berridge et al [19] compared ^{15}O-labeled butanol which has E = 1 [18] and ^{15}O-labeled water in the identical normal volunteers. Instead of Equation 19, they used the equation

$$Fcorr = F/[1-\exp(-PS/F)]. \qquad (20)$$

They calculated PS by a nonlinear regression fit of the corrected data of ^{15}O-labeled water with Equation 19 to the measured butanol, resulting in PS = 133 ml/min/100 g. With Equation 20, the corrected standard reference table Gscorr(C) is expressed as:

$$Gscorr(C) = \frac{Gs(C)}{1 - \exp\left[-\frac{PS}{F}\right]}$$: Extraction-corrected standard reference table

where F = Gs(C).

This approach may not be strictly precise, because a PS correction based on Equation 20 should be applied to the absolute CBF value. However, with the assumption that intrasubject and intersubject variability of global CBF is relatively small, and considering that Fs (50 ml/min/100 g) is close to the mean of the measured Fg (49.5 $\pm$ 7.9 ml/min/100 g), the correction might be justified.

In the corrected standard reference table Gscorr(C) and its increase propagation factors (Figure 3 and Table 4) , the PS value was assumed to be 133 ml/min/100 g [19]. Much more amplification of ΔC is achieved with the PS corrected standard reference table than with the uncorrected one. As this amplification is larger in the higher flow range, this correction would be of great help in detecting activated foci, which are expected to occur in the high flow region.

Our method cannot assess the changes in global CBF common to the non-invasive methods proposed previously [1,3]. Our approach requires strict control of the volume and speed of tracer injection. Further, a series of arterial sampling and injected dose measurements should be performed on normal subjects to acquire the standard arterial input function before any noninvasive studies are performed.

In conclusion, the standard arterial input function method is feasible for correcting the underestimation of relative changes in CBF in neurobehavioral task batteries. This method is particularly useful when the scanning time is relatively long, and when the analysis of the data is based on regional analysis.

ACKNOWLEDGMENT

The authors would like to thank Ms. B.J. Hessie for editorial assistance.

References

1. P. T. Fox, M. A. Mintun, M. E. Raichle, and P. Herscovitch, "A noninvasive approach to quantitative functional brain mapping with $H_2{}^{15}O$ and positron emission tomography,"J. Cereb. Blood Flow Metab. ,vol.4, pp.329-333,1984.

2. P. T. Fox, and M. A. Mintun, "Noninvasive functional brain mapping by change-distribution analysis of averaged PET images of $H_2{}^{15}O$ tissue activity,"J.Nucl. Med. , vol.30, pp.141-149,1989.

3. J. C. Mazziotta, S.-C. Huang, M. E. Phelps, R. E. Carson, N. S. MacDonald, and K. Mahoney, "A noninvasive positron computed tomography technique using oxygen-15-labeled water for the evaluation of neurobehavioral task batteries,"J. Cereb. Blood Flow Metab. ,vol.5, pp.70-78,1985.

4. I. Kanno, A. A. Lammertsma, J. D. Heather, et al., "Measurement of cerebral blood flow using bolus inhalation of $C^{15}O_2$ and positron emission tomography: description of the method and its comparison with the $C^{15}O_2$ continuous inhalation method.,"J. Cereb. Blood Flow Metab., vol.4, pp.224-234,1984.

5. I. Kanno, H. Iida, S. Miura, et al., "A system for cerebral blood flow measurement using $H_2{}^{15}O$ autoradiographic method and positron emission tomography,"J. Cereb. Blood Flow Metab., vol.7, pp.143-153,1987.

6. M.E. Raichle, W.R.W. Martin, P. Herscovitch, M.A. Mintun, and J. Markham, "Brain blood flow measured with intravenous $H_2{}^{15}O$. II, Implementation and validation," J. Nucl. Med., vol.24, pp. 790-798, 1983.

7. P.T. Fox, H. Burton, and M.E. Raichle, "Mapping human somatosensory cortex with positron emission tomography," J. Neurosurg.,vol.67,pp.34-43, 1987.

8. P.T. Fox, M.A. Mintun, M.E. Raichle, F.M. Miezin, J.M.Allman, and D.C. Van Essen, "Mapping human visual cortex with positron emission tomography," Nature, vol.323, pp. 806-809, 1986.

9. P.T. Fox, M.E. Raichle, "Stimulus rate dependence of regional cerebral blood flow in human striate cortex, demonstrated by positron emission tomography," J. Neurophysiol. vol.51,pp.1109-1120, 1984.

10. P.T. Fox, J.M. Fox, M.E. Raichle, and R.M. Burde, "The role of cerebral cortex in the generation of voluntary saccades: a positron emission tomographic study," J. Neurophysiol., vol.54, pp.348-369, 1985.

11. R.J. Seitz, and P.E. Roland, "Learning of sequential finger movements in man: a combined kinematic and positron emission tomography (PET) study," Eur. J. Neurosci., vol.4, pp.154-165, 1992.

12. P. Herscovitch, J. Markham, and M.E. Raichle, "Brain blood flow measured with intravenous $H_2{}^{15}O$. I. Theory and error analysis," J. Nucl. Med., vol.24, pp. 782-789, 1983.

13. H. Iida, I. Kanno, S. Miura, M. Murakami, K. Takahashi, and K. Uemura, "Error analysis of a quantitative cerebral blood flow measurement using $H_2{}^{15}O$

autoradiography and positron emission tomography, with respect to the dispersion of the input function," J. Cereb. Blood Flow Metab. ,vol.6, pp.536-545,1986.

14. T. Mukai, M. Senda, Y. Yonekura, et al. "System, design and performance of a newly developed high resolution PET scanner using double wobbling mode," J. Nucl. Med., vol.29, pp.877, 1988.

15. A.A. Lammertsma, and B.M. Mazoyer, "EEC concerted action on cellular degeneration and regeneration studied with PET. Modelling expert meeting blood flow measurement with PET - Orsay, 12-13 October 1989," Eur. J. Nucl. Med., vol.16, pp.807-812, 1989.

16. V. Dhawan, J. Conti, M. Mernyk, J.O.Jarden, D.A. Rottenberg, "Accuracy of PET RCBF measurements: effect of time shift between blood and brain radioactivity curves," Phys. Med. Biol., vol 31, pp.507-514,1986.

17. H. Iida, S. Higano, N. Tomura, et.al. "Evaluation of regional differences of tracer appearance time in cerebral tissues using ^{15}O-water and dynamic positron emission tomography," J. Cereb. Blood Flow Metab., vol.8, pp.285-288,1988.

18. P. Herscovitch, M.E. Raichle, M.R. Kilbourn, and M.J. Welch, "Positron emission tomographic measurement of cerebral blood flow and permeability-surface area product of water using [^{15}O] and [^{11}C] butanol," J. Cereb. Blood Flow Metab., vol.7, pp.527-542, 1987.

19. M.S. Berridge, L.P. Adler, A.D. Nelson, E.H. Cassidy, R.F. Muzic, E.M.Bednarczk, and F. Miraldi, "Measurement of human cerebral blood flow with [^{15}O]butanol and positron emission tomography," J. Cereb. Blood Flow Metab., vol.11, pp.707-715,1991.

Figure legends

FIGURE 1. Distribution of increase propagation factors $\hat{H}_{(x)}$. Variable x is the radiotracer concentration relative to the global mean of each measurement. Values are mean $\pm$ 1SD of 31 measurements.

FIGURE 2. Standard arterial input function obtained from 10 normal volunteers with dose calibration and peak time normalization.

FIGURE 3. Standard reference table with (open circles) and without (closed circles) correction of incomplete extraction of water. PS = 133 ml/min/100 g [16] was used.

Table 1. Increase propagation factors at tissue concentration of radiotracer relative to global mean from standard reference table ($\widehat{H}_s(x)$) vs from reference tables calculated with measured arterial input function ($\widehat{H}(x)$).

100x(%)	$\widehat{H}_s(x)$*	$\widehat{H}(x)$ (N = 31)		
		mean	SD	%Coef.var.(SD/mean x 100)
10	1.02	1.02	0.005	0.494
20	1.04	1.04	0.008	0.776
30	1.06	1.06	0.011	1.013
40	1.08	1.08	0.013	1.164
50	1.10	1.10	0.016	1.451
60	1.12	1.12	0.019	1.681
70	1.14	1.14	0.022	1.977
80	1.16	1.16	0.027	2.311
90	1.19	1.19	0.032	2.712
100	1.21	1.21	0.040	3.309
110	1.24	1.24	0.048	3.859
120	1.28	1.28	0.057	4.442
130	1.31	1.32	0.077	5.814
140	1.35	1.36	0.079	5.809
150	1.39	1.40	0.091	6.512

*When Cs = 237 nCi/ml.

Table 2. Systematic error of ΔFest and ΔC at various values of CBF (ml/min/100 g) where ΔF = 0.3.

CBF	ΔFest-ΔF	ΔC-ΔF
30	0.53 ±1.62	-3.97 ±1.36 *
50	0.00 ±1.17	-6.66 ±0.96 *
70	-0.58 ±2.13	-9.19 ±1.59 *

* $p < 0.01$ (ANOVA) for comparison with ΔFest-ΔF.

Table 3. Systematic error of ΔFest and ΔC at various values of ΔF(%) where F = 50 ml/min/100gr.

ΔF	ΔFest-ΔF	ΔC-ΔF
0.1	0.14 ± 1.71	-1.96 ± 0.84 *
0.2	-0.07 ± 0.88	-4.24 ± 0.79 *
0.3	0.00 ± 1.17	-6.66 ± 0.96 *
0.4	-0.26 ± 1.34	-9.58 ± 1.46 *

* $p < 0.01$ (ANOVA) for comparison with ΔFest-ΔF.

Table 4. Increase propagation factors at tissue concentration of radiotracer relative to global mean, with and without PS correction.

100x(%)	$\hat{H}_s(x)^*$	$\hat{H}_s(x)$PS corrected+
10	1.02	0.99
20	1.04	1.03
30	1.06	1.06
40	1.08	1.10
50	1.10	1.14
60	1.12	1.18
70	1.14	1.23
80	1.16	1.29
90	1.19	1.36
100	1.21	1.44
110	1.24	1.53
120	1.28	1.63
130	1.31	1.74
140	1.35	1.85
150	1.39	1.97

*When Cs = 237 nCi/ml.

+ With assumption that gCBF value is 50 ml/min/100 g, correction for incomplete extraction was performed. Mean PS value =133 ml/min/100 g [19].

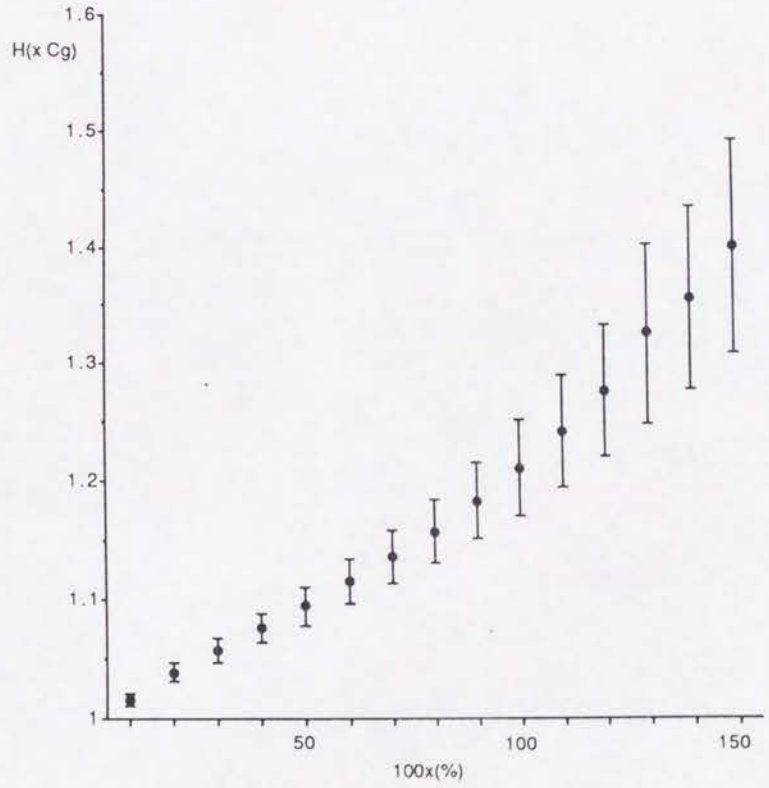

Figure 1

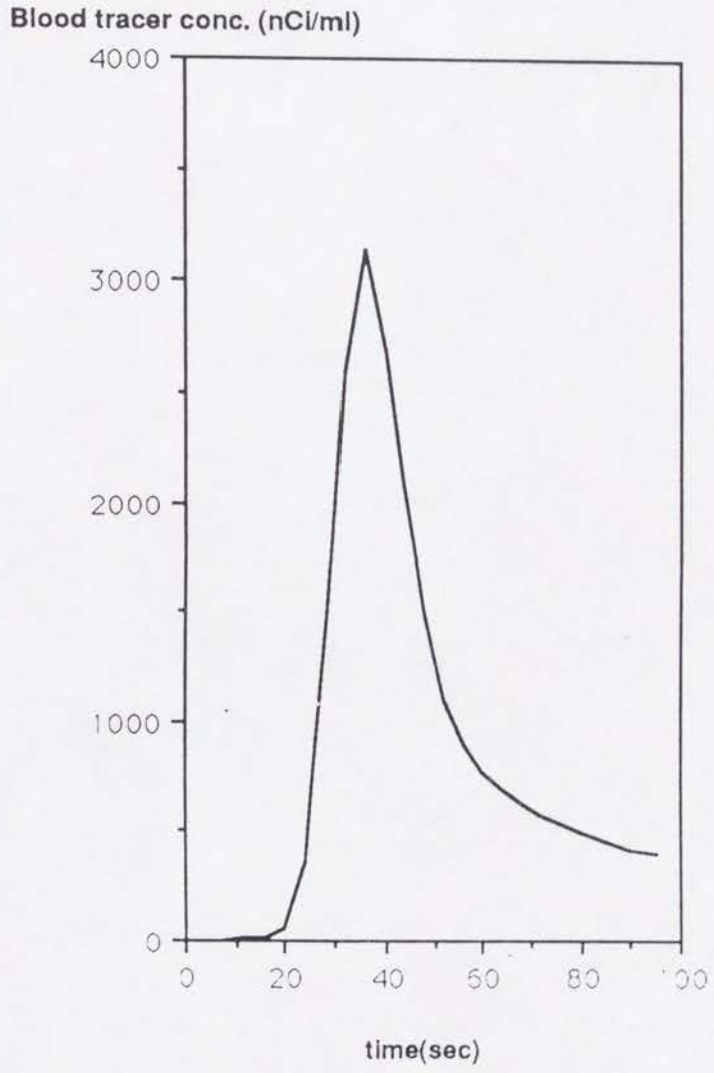
Blood tracer conc. (nCi/ml)
4000
3000
2000
1000
0
0
20
40
50
80
00
time(sec)

Figure 2

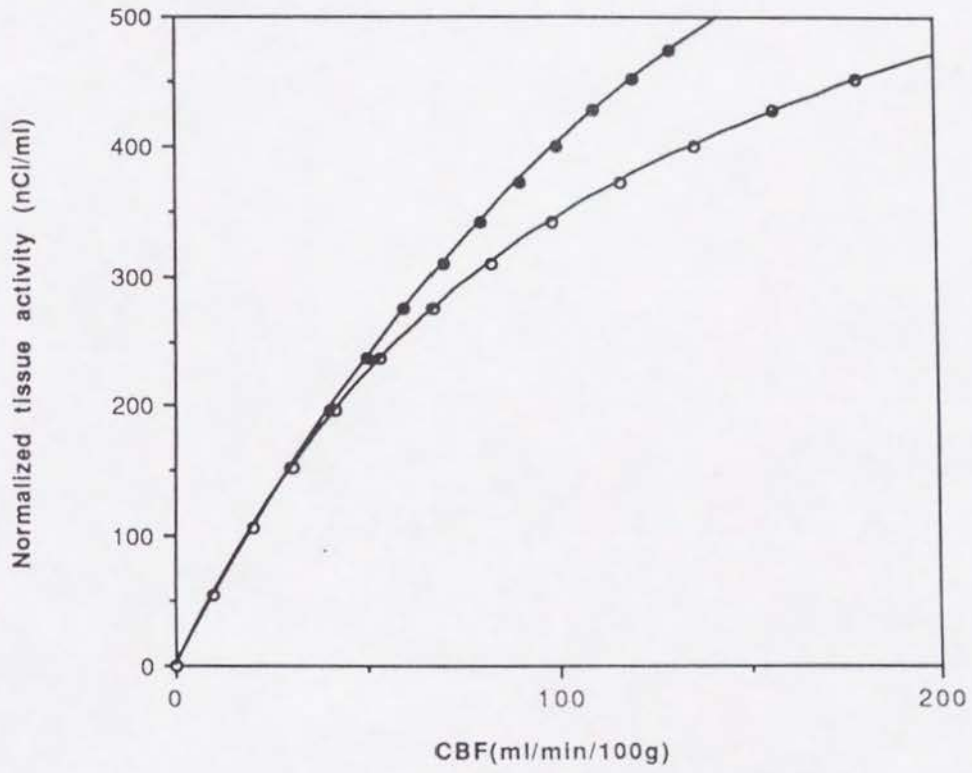
Normalized tissue activity (nCi/ml)
500
400
300
200
100
0
0
100
200
CBF(ml/min/100g)

Figure 3

Positron Emission Tomography and the Autoradiographic Method with Continuous Inhalation of ^{15}O Gas: Theoretical Analysis and Comparison with Conventional Steady-State Method

Norihiro Sadato, MD

Yoshiharu Yonekura, MD*

Michio Senda, MD **

Yasushi Iwasaki, MD

Naoki Matoba, MD

Nagara Tamaki, MD

Satoshi Sasayama, MS

Yasuhiro Magata, PhD

Junji Konishi, MD

Departments of Nuclear Medicine and *Brain Pathophysiology, Kyoto University Faculty of Medicine , Kyoto, Japan, and **Tokyo Metropolitan Institute of Gerontology, Tokyo, Japan

For correspondence: Norihiro Sadato, MD

Department of Nuclear Medicine, Kyoto University Faculty of Medicine

54 Kawahara cho, Shogoin, Sakyo ku, Kyoto, 606-01, Japan

Telephone: 81-75-751-3419

FAX: 81-75-751-3217

Running title:

PET/autoradiographic method with ^{15}O gas.

ABSTRACT

The steady-state method using ^{15}O gas inhalation and positron emission tomography (PET) is a simple and practical way of imaging cerebral blood flow (CBF) and oxygen metabolism. It has several disadvantages, however, such as prolonged examination time, the requirement of steady state, and a large tissue heterogeneity effect. To avoid the drawbacks of the steady-state method but preserve its simplicity, we applied the PET/autoradiographic method to the build-up phase during the continuous inhalation of ^{15}O gas with intermittent arterial sampling. A simulation study was performed to determine the optimal scanning period, evaluate the delay and dispersion effect of the input function, and estimate the tissue heterogeneity effect. To assess the clinical feasibility of the proposed technique for the study of oxygen metabolism, sequential measurements with the new method and the conventional steady-state method were performed in 8 patients. The simulation study showed that a 5-min scan started 3 min after the commencement of ^{15}O gas inhalation was optimal. With the new method, the delay and dispersion effect on CBF was the same as that of the conventional steady-state method, but the tissue heterogeneity effect was reduced. In 8 patients, CBF values calculated by the new method showed time dependency and were slightly higher than those obtained by the steady-state method. The oxygen extraction fraction showed no significant time dependency and was well correlated with that obtained by the steady-state method. We conclude that the proposed method is a simple and acceptable alternative to the conventional steady-state method.

INTRODUCTION

The continuous inhalation of ^{15}O labeled CO_2 and O_2 (steady-state method) is widely used as a simple and practical method to measure regional cerebral blood flow (CBF), oxygen extraction fraction (OEF), and cerebral metabolic rate of oxygen consumption ($CMRO_2$) by positron emission tomography (PET) (*1*). The method, however, has several disadvantages (*2-5*). The relatively long inhalation period required to achieve steady state (approximately 8 to 10 min) exposes subjects to a high level of radiation. Practically, it is difficult to determine the time when the tracer concentration has reached the steady state. Fluctuation of arterial activity may lead to substantial error in the calculated values, which cannot be completely corrected by averaging techniques (*2*). Finally, the steady-state method is subject to the effect of tissue heterogeneity (*5-7*).

The examination time was shortened by the introduction of an autoradiographic method directly based on Kety's one compartment model (*8*) without assuming steady state (*6, 9, 10*). Recently, a combination of dynamic and autoradiographic methods was also applied in $C^{15}O_2$ inhalation studies (*11-13*). These methods are less subject to the effect of tissue heterogeneity, but are more affected by delay and dispersion problems (*11, 12, 14*). Rapid separation of plasma is also required for calculation of the OEF (*10*).

Senda et al. (*2*) applied the autoradiographic method to correct the variation in arterial radioactivity concentration in the near steady state. Compared with the conventional steady-state method, this method can provide more robust parameters despite fluctuation of the arterial input function. However, it has the same disadvantages as the conventional method, that is, prolonged examination time and tissue heterogeneity effect . Because the algorithm of their method was similar to that used in the bolus injection of $H_2^{15}O$, it is applicable to the earlier phases in the gas inhalation method, resulting in faster examination and efficient

use of the administered radiation dose. Considering the longer build-up phase during continuous inhalation of gas than during bolus administration, a reasonable compromise between accuracy of the parameters and simplicity of the procedure would seem to be possible.

The purpose of this study was to apply the autoradiographic method to the build-up phase while preserving the simplicity of the steady-state method.

MATERIALS AND METHODS

Formulas for calculation

Formulas of the new method and the steady-state method are described in the Appendix.

CBF measurement with $C^{15}O_2$ inhalation

The regional change in cerebral radiotracer concentration during $C^{15}O_2$ inhalation is described as

$$\frac{dC_T(t)}{dt} = FC_a(t) - \frac{F\,C_T(t)}{p} - \lambda C_T(t) = FC_a(t) - (\frac{F}{p} + \lambda)C_T(t)$$

where $C_T(t)$ is the tissue concentration of $H_2{}^{15}O$, $C_a(t)$ is the arterial concentration of $H_2{}^{15}O$, F is the regional blood flow, p is the partition coefficient of water between brain and blood, assumed as unity in this study , and λ is the physical decay constant of ^{15}O.

In the steady state, where $dC_T(t)/dt = 0$,

$$F = \frac{\lambda}{\frac{C_a}{C_T} + \frac{1}{p}}$$

In the new method, PET value T from t_1 to t_2 is:

$$T = \frac{1}{t_2 - t_1}\int_{t_1}^{t_2} k_1 C_a(t) * e^{-k_2 t} dt$$

where * indicates convolution,

$$k_1 = F,$$
$$k_2 = \frac{F}{p} + \lambda,$$

assuming $C_T(t) = 0$.

This equation can be used to generate a lookup table, F = G(T), that relates T to F, from which CBF is estimated.

OEF measurement with $^{15}O_2$ inhalation

The regional change in cerebral parenchymal radiotracer concentration during $^{15}O_2$ inhalation is:

$$\frac{dC_t(t)}{dt} = FEC_o(t) + FC_H(t) - (\frac{F}{p} + \lambda)C_t(t)$$

where E is the oxygen extraction fraction(OEF),

Co(t) is the arterial concentration of $^{15}O_2$, and

$C_H(t)$ is the arterial concentration of $H_2{}^{15}O$.

In the steady state,

$$E = \frac{C_T(\frac{F}{p} + \lambda) - FC_H - V_bC_O(\frac{F}{p} + \lambda)}{pC_O - V_bC_O(\frac{F}{p} + \lambda)}$$

where V_b is the regional blood volume.

In the new method,

$$E = \frac{\hat{C}_T - (C_1 + C_3)}{C_2 - C_1}$$

where $\hat{C}_T$ is PET value from t_1 to t_2,

$$C_1 = \frac{1}{t_2 - t_1}\int_{t_1}^{t_2} V_bC_O(t)dt$$

$$C_2 = \frac{1}{t_2 - t_1}\int_{t_1}^{t_2} FC_O(t) * e^{-k_2t}dt$$

$$C_3 = \frac{1}{t_2 - t_1}\int_{t_1}^{t_2} FC_H(t) * e^{-k_2t}dt$$

Tomograph characteristics

The PCT-3600W system (Hitachi Medical Co., Tokyo, Japan) was employed for PET scanning (15,16). This system simultaneously acquires 15 slices with a center-to-center distance of 7 mm. All scans were performed at a resolution of 9 mm full width at half maximum (FWHM) in the transaxial direction and 6.5 mm in the axial direction. Field of view and pixel size of the reconstructed images were 256 mm and 2 mm, respectively. A transmission scan was obtained before all emission measurements.

Subjects

We studied 8 patients, aged 45 to 70 years, who had cerebral infarction (6 cases), dementia of the Alzheimer type (2 cases), Binswanger's disease (1 case), and epilepsy (1 case). Informed consent was obtained from each subject using forms and procedures approved by the Ethical Committee of the Kyoto University Faculty of Medicine. The subject's head was immobilized with head holders. A small catheter was placed in the brachial artery for blood sampling. The subject wore a light, disposable, plastic mask and a nasal cannula through which he breathed $C^{15}O$, $C^{15}O_2$ and $^{15}O_2$ produced by a small cyclotron (CYPRIS MODEL 325; Sumitomo Heavy Industries, Tokyo, Japan).

Tracer techniques

CBV study

To obtain the fractional regional cerebral blood volume (CBV), bolus inhalation of $C^{15}O$ with 3-min scanning was performed. Arterial samples were obtained manually twice during the scanning for calculation of CBV using the following formula:

$$CBV = \frac{PET}{R\,D\,\overline{C}_A}\,100$$

where PET is the PET value, $\overline{C}_A$ is the mean of the decay-corrected radiotracer concentration in arterial blood, R is the mean ratio of the small-vessel to large-vessel hematocrit, equal to 0.85, and D is the density of brain tissue, equal to 1.05 g/ml (10).

CBF and OEF study

The subjects inhaled a steady supply of tracer amounts of $^{15}O_2$ for 18 min (Fig. 1). Scanning was started simultaneously with the commencement of $^{15}O_2$ inhalation. Dynamic scans of 18 consecutive frames (1 frame/min) were obtained. After a 15-min intermission, $C^{15}O_2$ was inhaled for 18 min for more dynamic scans with the same protocol.

Arterial blood was sampled manually from the brachial artery at 20 sec, 40 sec, 60 sec, 2 min, 4 min, 6 min,8 min,10 min, 12 min,14 min, 16 min, and 18 min after the commencement of inhalation. Each sample was collected for 10 to 20 sec to average the fluctuations due to the respiratory cycle (*2, 17*), and activity of radiotracer concentrations in whole blood and plasma was measured with a well counter. Arterial hematocrit, PaO_2, $PaCO_2$, and arterial hemoglobin were also measured.

Data processing

The arterial activity curves were determined with interpolation between the measured points. The reconstructed dynamic images of frames 5-8 and 9-13 were added to make the late build-up phase images and near steady-state images, respectively. For the conventional steady-state method, near steady-

state images and averaged arterial activities were used. For the new method, both late build-up and near steady-state phase images were used to evaluate the time dependency of the calculated parameters.

Data analysis

Profiles of input functions

To assess the profile of the input functions $C_a(t)$, $C_O(t)$ and $C_H(t)$ from the 8 patients, each arterial input function was normalized with the mean arterial concentration of the presumed steady-state phase (10-18 min). The mean and standard deviation of 8 curves were plotted at each measurement point (Fig. 2).

Simulation study

A simulation study was performed with typical arterial input functions approximated by the exponential equations:

$C_a(t) = 1067(1- \exp[-t/110])$

$C_O(t) = 1250(1- \exp[-t/50])$

$C_H(t) = 400(1- \exp[-t/200])$

The weight contribution of the early build-up phase on the calculated parameters was assessed. Consider the $C^{15}O_2$ inhalation study. If $u < t$, the weight contribution of $C_a(u)$ from $u = 0$ to t_a on PET value T is a function of t_a:

$$h(t_a) = \frac{\int_{t_1}^{t_2} \int_0^{t_a} C_a(u)e^{-k_2(t-u)}dudt}{\int_{t_1}^{t_2} \int_0^{t} C_a(u)e^{-k_2(t-u)}dudt}$$

If $h(t_a)$ is sufficiently small, the influence of $C_a(t)$ (t = 0 to ta) on the PET value can be ignored. The weight contribution of $C_O(t)$ on C_2 and $C_H(t)$ on C_3 was also evaluated.

The effect of the delay and dispersion of the input function was evaluated. The measured arterial radioactivity is delayed and dispersed with respect to the cerebral arterial activity (*11,14*). The effect on the calculated CBF was estimated using the following equation. The measured input function $C_a(t)$ is expressed with the true input function $C_a^0(t)$ as:

$$C_a(t + d)\, e^{\lambda d} = C_a^0(t) * \left(\frac{e^{-(\frac{1}{\tau} + \lambda)\tau}}{\tau}\right)$$

where the dispersion function is assumed as $\frac{1}{\tau}\exp[\frac{-t}{\tau}]$ (*11,14*) , and d is delay of the measured arterial curve. True tissue activity $C_T(t)$ and PET value T are expressed as:

$$C_T(t) = FC_a(t+d)\exp[\lambda d]\tau + FC_a(t+d)\exp[\lambda d](1-\tau F/p) * \exp[-(F/p+\lambda)t]$$

$$T = \frac{1}{t_2-t_1}\int_{t_1}^{t_2} C_T(t)dt$$

When d and τ are known, the unique flow F can be calculated by the lookup table method:

$$F = G_{d,\tau}(T)$$

where $G_{d,\tau}(T)$ is a lookup table with the correction for delay and dispersion.

As our method assumes both d and t as null, % error of calculated flow due to delay and dispersion is estimated as:

$$\%\ \text{error in flow} = \frac{G_{0,0}(G_{d,\tau}^{-1}(F)) - F}{F}\ 100$$

The same evaluation was performed on the conventional steady-state method. In the case of the constant input function,

$$C_a(t) = C_a,\quad C_a^0(t) = C_a^0$$

$$C_a^0 = e^{\lambda d}\,(1 + \lambda\tau)\,C_a$$

Measured CBF F_d and true CBF F are:

$$F_d = \frac{\lambda}{\frac{C_a}{C_T} - 1}$$

$$F = \frac{\lambda}{e^{\lambda d}\,(1 + \lambda\tau)\frac{C_a}{C_T} - 1}$$

$$\%\ \text{error in flow} = \frac{F_d - F}{F}\ 100 = \left(\frac{\lambda}{\frac{e^{-\lambda d}\,(F + \lambda)}{(1 + \lambda\tau)} - F} - 1\right) 100$$

The effect of tissue heterogeneity on CBF measurement was assessed with the late build-up phase and the steady-state phases. Error in measured flow was calculated for a region of interest (ROI) containing varying proportions of two tissues with equal partition coefficients of 1 ml/g, but with different flows, assuming 20 ml/min/100 g for white matter and 80 ml/min/100 g for gray matter. Per cent underestimation was calculated with the following equation:

$$\%\ \text{underestimation} = \frac{g\alpha + w(1-\alpha) - G(G^{-1}(g)\alpha + G^{-1}(w)(1-\alpha))}{g\alpha + w(1-\alpha)} \times 100$$

where G is a lookup table from tissue activity to flow, g is the CBF value of gray matter, w is the CBF value of white matter, and α is the proportion of gray matter in a ROI.

The statistical noise of CBF images obtained with the new method was compared between the build-up phase and the near steady-state phase. In the latter phase, there was a tradeoff between better count statistics and more noise propagation due to a larger nonlinearity in the count-flow relationship. The statistical error in CBF(ΔCBF/CBF) was estimated as:

$$\frac{\Delta CBF}{CBF} = \frac{\frac{\partial f}{\partial T}}{\frac{f}{T}} \frac{\Delta T}{T}$$

where

$\frac{\partial f}{\partial T}$ is the slope of the lookup table (*18*). The term $\frac{\frac{\partial f}{\partial T}}{\frac{f}{T}}$ is an error propagation factor from tissue count rate to flow, indicating nonlinearity in the count-flow relationship. The statistical noise of the integration (ΔT) was estimated using the statistical relationship $\Delta T \propto \sqrt{T}$ (*18*).

Validation study

With the data obtained from the 8 patients, CBF and OEF images were calculated with the conventional steady-state method and the new method. The new method was applied to both the late build-up phase and the near-steady-state phase. The conventional steady-state method was applied to the near steady-state phase. Whole brain ROIs were taken in the slices 84 mm above the orbitomeatal line, including mainly the centrum semiovale, to analyze systematic differences in the calculations. ROIs were defined in $C^{15}O_2$ tissue activity images of the near steady-state and projected on the parametric images. When the slices showed infarction, slices from the normal hemisphere were used.

RESULTS

Profiles of input function

During $C^{15}O_2$ inhalation, arterial radiotracer activity rose steeply during the first minute, gradually increased from 1 to 8 min, and reached steady state approximately 8 min. During $^{15}O_2$ inhalation, the arterial concentration of $^{15}O_2$ rose rapidly during the first 2 min and reached steady state at approximately 4 min, although fluctuation of $\pm$ 10 % was observed during the later phase. The concentration of $H_2{}^{15}O$ gradually increased during the first 10 min, and reached steady state later (Fig. 2).

Simulation study of parameter calculation

Weight contribution of early build-up phase

Table 1 shows the weight contribution of the early build-up phase on the input functions on T, C_2, and C_3 when the scans were performed at the late build-up phase. The weight contribution of the first 1 min was as small as 1%.

Delay and dispersion effect

Delay and dispersion effects on CBF were equivalent between the methods (Table 2). When the delay was 5 sec, overestimation of the calculated CBF at 50 ml/min/100 g was approximately 7%. A 5-sec delay was equivalent to a 2.5-sec delay plus a 2.5-sec dispersion (Table 2).

Tissue heterogeneity effect

Figure 3 shows error propagation factors plotted against CBF. Nonlinearity between flow and tissue activity is most prominent in the conventional steady-state method, less prominent in the new method at near steady state, and least prominent in the new method at the late build-up phase.

Figure 4 shows the tissue heterogeneity effect on CBF by the new method with different scanning periods. Underestimation of CBF was less prominent with the late build-up phase (3-8 min scan) than with the steady-state phase (8 -13 min scan and 13-18 min scan). The tissue heterogeneity effect was equivalent with the conventional steady-state method and the new method when the same scanning period (8 -13 min) was used.

Statistical errors of CBF

Statistical errors of CBF, $\Delta CBF/CBF$, calculated with the build-up method using the late build-up phase and the near steady-state phase were equivalent (Table 3).

Validation study

Table 4 shows the comparison between the new method and the conventional steady-state method in 8 patients. Because the whole brain contains a mixture of gray matter, white matter, cerebrospinal fluid, and possibly lesions, the differences in the parameter estimates between the two methods indicate the overall effect by the new method (2). Time dependency of CBF values was observed ($P < 0.01$, ANOVA). CBF values calculated with the late build-up phase was 11% higher than those with the near steady-state phase (8-13 min). CBF values calculated with the near steady-state phase in the build-up method were 2% higher than those with the conventional steady-state method, but the difference was not significant. No time dependency of OEF values was observed ($P > 0.8$, ANOVA). OEF values calculated with the build-up method and the conventional steady-state method were equivalent.

DISCUSSION

Our method is categorized as an autoradiographic method with ramped input function. Iida et al. (*18*) performed a systematic study of the shape of the input function and the duration of the scan in the autoradiographic method for CBF measurement . The bolus method, with sharp peaks and short scanning duration, is sensitive to delay and dispersion, but provides a linear count-flow relationship with less tissue heterogeneity effect. Dead-time error and accidental coincidence could be a problem. Because of the short scanning period, the calculated CBF is likely to fluctuate. In contrast, the ramped input function allows a longer scan duration, resulting in less sensitivity to delay and dispersion, and a larger nonlinearity, causing more effect of tissue heterogeneity. There is no dead-time problem. By administering sufficient amounts of $H_2{}^{15}O$ and scanning for a long period, the statistical error in CBF may be negligible. The contribution weights cover the whole scan period, providing more stable CBF values (*18*).

To apply the autoradiographic method to the build-up phase, preserving the simplicity of the conventional steady-state method, we first analyzed the profiles of input function to determine the optimal scan period. $C_a(t)$ and $C_O(t)$ showed a rapid rise in the first 2 min, later forming a gradual build-up phase. $C_H(t)$ showed a gradual increase in the first 10 min, while the absolute value was relatively small. Rapid change of or low radiotracer concentration in whole blood or plasma during the earlier build-up phase could cause measurement error. Additionally, in the gas inhalation study, the respiratory cycle may cause variation in the tissue as well as arterial activity, particularly in elderly and diseased populations (*2*). These factors are accentuated with intermittent arterial sampling because of the limited sampling interval. For these reasons, the early build-up phase is not suitable for the scanning period.

The tissue radiotracer concentration is determined not only by the current arterial concentration but also by its weighted integral (convolution) during the preceding several minutes, unless steady state is achieved and maintained (*2*). When the late build-up phase (3-8 min) is adopted for the scanning period, calculated parameters of T, C_2 and C_3 are minimally affected by the input functions of the first 1 to 2 min. Because $C_a(t)$ and $C_O(t)$ rises steeply in the first 1 to 2 min, but later becomes less (Fig. 2), intermittent blood sampling at intervals of 1 to 2 min would be sufficient, and input functions would be interpolated, assuming tissue radiotracer concentration at t = 0 is 0.

Correction of delay and dispersion of arterial input function is essential for accurate estimation of CBF (*11,14,18*). In this study, however, the correction was not performed for the following reasons. First, we adopted manual arterial sampling, in which external delay and dispersion were negligible. Second, it is impossible to measure the internal delay time and dispersion constant with the single-frame autoradiographic method. With the dynamic method, mean internal dispersion time is estimated at 5 sec if blood is sampled at the radial artery (*14*), and differences of arrival time (" head-to-hand " time lag) are 3 sec (*19*). However, the correction is not practical, as internal delay and dispersion depend on the site of arterial sampling (radial artery vs brachial artery) and on the location of the brain region (*20*). Third , the steady-state method is also subject to a delay and dispersion effect because of the short half life of ^{15}O ($T_{1/2}$ = 123 sec). A 5-sec delay of arterial input function causes approximately a 3% decrease of the radiotracer activity, resulting in 7.4% overestimation of CBF at 50 ml/min/100 g. This overestimation has not usually been corrected (*1*). Lastly, as shown in Table 2, the delay and dispersion effect in the late build-up phase was as small as that in the near steady-state phase (8-13 min) and in the later steady-state phase (13-18 min) with the same scan duration.

The limited resolution of the PET scanner and the nonlinear count-flow relationship (Fig. 3) cause systematic underestimation of CBF (*21*). With the build-up method, the underestimation of CBF because of flow heterogeneity was larger in the near steady-state phase than in the late build-up phase (Fig. 4). In this study, the heterogeneity of partition coefficient was not considered, because the new method was designed to improve the conventional steady-state method, which usually uses the fixed value of partition coefficient of water (*1, 2*).

As shown in Table 4, CBF values calculated with the build-up method using the late build-up phase were higher than those using the near steady-state phase. This time dependency of CBF is caused by delay and dispersion of the input function, as well as by the tissue heterogeneity effect (*12, 14*). As the former factor has the same effect in both the late build-up phase and the steady-state phase (Table 2), the tissue heterogeneity effect would be the main cause. Considering the diseases and older ages of our subjects, the effect of nonperfusable space might be large. In contrast, our method provided OEF values equivalent to those with the conventional steady-state method without time dependency. As expected from equation (15) in the Appendix, OEF is mainly determined as the ratio of $\widehat{C_t}$ and C_2, where time dependency might be canceled out.

In conclusion, our method is a simple and practical alternative to the conventional steady-state method for obtaining images of oxygen metabolism.

APPENDIX

The algorithm of the new method was presented by Senda et al. (*2*).

CBF measurement with $C^{15}O_2$ inhalation

CBF measurement was performed with an adaptation of Kety's diffusible autoradiographic method (*8*). The regional change in cerebral radiotracer concentration during $C^{15}O_2$ inhalation is described as

$$\frac{dC_T(t)}{dt} = FC_a(t) - \frac{F\,C_T(t)}{p} - \lambda C_T(t) = FC_a(t) - (\frac{F}{p} + \lambda)C_T(t) \qquad (1)$$

where $C_T(t)$ is the tissue concentration of $H_2{}^{15}O$, $C_a(t)$ is the arterial concentration of $H_2{}^{15}O$ measured by blood sampling, F is the regional blood flow, p is the partition coefficient of water between brain and blood, and λ is the physical decay constant of ^{15}O.

In the steady state, where $dC_T(t)/dt = 0$,

$$F = \frac{\lambda}{\frac{C_a}{C_T} + \frac{1}{p}} \qquad (2)$$

In the new method, $C_T(t)$ and $C_a(t)$ need not be constant.

$$C_T(t) = k_1 C_a(t) * e^{-k_2 t} \qquad (3)$$

where * indicates convolution,

$$k_1 = F,$$
$$k_2 = \frac{F}{p} + \lambda$$

assuming $C_T(t) = 0$.

PET value T obtained from the scan from t_1 to t_2 is,

$$T=\frac{1}{t_2 - t_1}\int_{t_1}^{t_2} C_T(t)dt \qquad (4)$$

The arterial activity curve $C_a(t)$ is determined by multiple blood sampling starting from the commencement of inhalation with interpolation between measured points to create a smooth curve. A lookup table, F = G(T), is then generated to relate T to F, from which CBF is estimated.

OEF measurement with $^{15}O_2$ inhalation

Tissue radiotracer concentration $C_T(t)$ is the sum of the tissue activity in proper $C_t(t)$ and the blood pool activity $C_b(t)$:

$$C_T(t) = C_t(t) + C_b(t) \qquad (5)$$

The regional change in cerebral parenchymal radiotracer concentration during $^{15}O_2$ inhalation is:

$$\frac{dC_t(t)}{dt} = FEC_o(t) + FC_H(t) - \frac{F\,C_t(t)}{p} - \lambda C_t(t)$$
$$= FEC_o(t) + FC_H(t) - (\frac{F}{p} + \lambda)C_t(t) \qquad (6)$$

where E is the oxygen extraction fraction(OEF),

Co(t) is the arterial concentration of $^{15}O_2$,

$C_H(t)$ is the arterial concentration of $H_2{}^{15}O$, calculated from the activity of whole blood and plasma with $C^{15}O_2$ and $^{15}O_2$ inhalation, assuming that all the activity in the plasma comes from $H_2{}^{15}O$(*2*).

$$C_H(t) = A\,C_P(t) \qquad (7)$$

where

A = (water content of whole blood)/(water content of plasma) and

$C_P(t)$ is $H_2{}^{15}O$ activity in plasma.

Constant A can be derived if the packed cell volume (PCV) of the arterial blood is measured and the ratio of water between red cells and plasma is assumed constant (*1*).

$A=1 - 0.245\ PCV$

$$C_O(t) = C_A(t) - C_H(t) \tag{8}$$

where $C_A(t)$ is ^{15}O activity in whole blood.

$$C_t(t) = (FEC_O(t) + FC_H(t)) * e^{-k_2 t} \tag{9}$$

where $k_2 = \frac{F}{p} + \lambda$.

The regional radiotracer concentration in the vascular component $C_b(t)$ is

$$C_b(t) = V_b(1-E)C_O(t) \tag{10}$$

where V_b is the fractional blood volume.

In the steady state, all variables are time-independent.

$$C_T = C_t + C_b = \frac{FEC_O + FC_H}{\frac{F}{p} + \lambda} + V_b(1 - E)C_O \tag{11}$$

or

$$E = \frac{C_T(\frac{F}{p} + \lambda) - FC_H - V_bC_O(\frac{F}{p} + \lambda)}{pC_O - V_bC_O(\frac{F}{p} + \lambda)} \tag{12}$$

In the new method,

$$C_T(t) = C_t(t) + C_b(t)$$

$$= (FEC_O(t) + FC_H(t)) * e^{-k_2 t} + V_b(1-E)C_O(t)$$

$$= E(FC_O(t) * e^{-k_2 t} - V_bC_O(t)) + FC_H(t) * e^{-k_2 t} + V_bC_O(t) \tag{13}$$

PET value obtained from t_1 to t_2 is:

$$\hat{C}_T = \frac{1}{t_2 - t_1}\int_{t_1}^{t_2} C_T(t)dt$$

$$= \frac{1}{t_2 - t_1}\int_{t_1}^{t_2} \{E(FC_O(t) - V_bC_O(t)) + FC_H(t)) * e^{-k_2t} + V_bC_O(t)\}dt$$

$$E = \frac{-\int_{t_1}^{t_2} \{FC_H(t) * e^{-k_2t} + V_bC_O(t)\}dt + (t_2 - t_1)\hat{C}_T}{\int_{t_1}^{t_2} \{FC_O(t) * e^{-k_2t} - V_bC_O(t)\}dt} \quad (14)$$

Or, $$E = \frac{\hat{C}_T - (C_1 + C_3)}{C_2 - C_1} \quad (15)$$

where

$$C_1 = \frac{1}{t_2 - t_1}\int_{t_1}^{t_2} V_bC_O(t)dt \quad (16)$$

$$C_2 = \frac{1}{t_2 - t_1}\int_{t_1}^{t_2} FC_O(t) * e^{-k_2t}dt \quad (17)$$

$$C_3 = \frac{1}{t_2 - t_1}\int_{t_1}^{t_2} FC_H(t) * e^{-k_2t}dt \quad (18)$$

The arterial blood is sampled several times during the study starting from t = 0 to obtain the $C_O(t)$ and $C_H(t)$.

ACKNOWLEDGMENT

The authors would like to thank Ms. B.J. Hessie for editorial assistance.

REFERENCES

1. Frackowiak RSJ, Lenzi G, Jones T, Heather JD. Quantitative measurement of regional cerebral blood flow and oxygen metabolism in man using ^{15}O and positron emission tomography : theory, procedure, and normal values. *J Comput Assist Tomogr* 1980;4:727-736.

2. Senda M, Buxton RB, Alpert NM, et al. The ^{15}O steady state method: correction for variation in arterial concentration. *J Cereb Blood Flow Metab* 1988;8:681-690.

3. Lammertsma AA, Heather JD, Jones T, Frackowiak RSJ, Lenzi G. A statistical study of the steady state technique for measuring regional cerebral blood flow and oxygen utilisation using ^{15}O. *J Comput Assist Tomogr* 1982;6:566-573.

4. Jones SC, Greenberg JH, Reivich M. Error analysis for the determination of cerebral blood flow with the continuous inhalation of ^{15}O labeled carbon dioxide and positron emission tomography. *J Comput Assist Tomogr* 1982;6:116-124.

5. Correia JA, Alpert NM, Buxton RB, Ackerman RH. Analysis of some errors in the measurement of oxygen extraction and oxygen consumption by the equilibrium inhalation method. *J Cereb Blood Flow Metab* 1985;5:591-599.

6. Herscovitch P, Raichle ME. Effect of tissue heterogeneity on the measurement of cerebral blood flow with the equilibrium $C^{15}O_2$ inhalation technique. *J Cereb Blood Flow Metab* 1983;3:407-415.

7. Huang S, Mahoney DK, Phelps ME. Quantitation in positron emission tomography 8. Effects of nonlinear parameter estimation on functional images. *J Comput Assist Tomogr* 1987;11:314-325.

8. Kety SS. The theory and applications of the exchange of inert gas at the lungs and tissues. *Pharmacol Rev* 1951;3:1-41.

9. Raichle ME, Martin WRW, Herscovitch P, Mintun M, Markham J. Brain blood flow measured with intravenous $H_2{}^{15}O$. II. Implementation and validation. *J Nucl Med* 1983;24:790-798.

10. Mintun MA, Raichle ME, Martin WRW, Herscovitch P. Brain oxygen utilization with O-15 radiotracers and positron emission tomography. *J Nucl Med* 1984;25:177-187.

11. Lammertsma AA, Frackowiak RSJ, Hoffman JM, et al. The $C^{15}O_2$ build-up technique to measure regional cerebral blood flow and volume of distribution of water. *J Cereb Blood Flow Metab* 1989;9:461-470.

12. Lammertsma AA, Cunningham VJ, Deiber MP, et al. Combination of dynamic and integral methods for generating reproducible functional CBF images. *J Cereb Blood Flow Metab* 1990;10:675-686.

13. Lammertsma AA, Martin AJ, Friston KJ, Jones T. In vivo measurement of the volume of distribution of water in cerebral grey matter: Effects on the calculation of regional cerebral blood flow. *J Cereb Blood Flow Metab* 1992;12:291-295.

14. Iida H, Kanno I, Miura S, Murakami M, Takahashi K, Uemura K. Error analysis of a quantitative cerebral blood flow measurment using $H_2{}^{15}O$ autoradiography and positron emission tomography, with respect to the dispersion of the input function. *J Cereb Blood Flow Metab* 1986;6:536-545.

15. Mukai T, Senda M, Yonekura Y, et al. System, design and performance of a newly developed high resolution PET scanner using double wobbling mode. *J Nucl Med* 1988;29:877.

16. Endo M, Hukuda H, Suhara T, et al. Design and performance of PCT-3600w (15-slice type): a whole-body positron emission tomograph. *J Nucl Med* 1988;32:1061

17. Meyer E, Yamamoto YL. The requirement for constant arterial radioactivity in the $C^{15}O_2$ steady-state blood-flow model. *J Nucl Med* 1984;25:455-460.

18. Iida H, Kanno I, Miura S. Rapid measurement of cerebral blood flow with positron emission tomography. In: Chadwick DJ, Whelan J, eds. 1991 Exploring brain functional anatomy with positron tomography. Chichester: Wiley; 1991: 23-42.

19. Dhawan V, Conti J, Mernyk M, Jarden JO, Rottenberg DA. Accuracy of PET RCBF measurements: effect of time shift between blood and brain radioactivity curves. *Phys Med Biol* 1986;31:507-514.

20. Iida H, Higano S, Tomura N, et al. Evaluation of regional differences of tracer appearance time in cerebral tissues using ^{15}O-water and dynamic positron emission tomography. *J Cereb Blood Flow Metab* 1988;8:285-288.

21. Iida H, Kanno I, Miura S, Murakami M, Takahashi K, Uemura K. A determination of the regional brain/blood partition coefficient of water using dynamic positron emission tomography. *J Cereb Blood Flow Metab* 1989;9:874-885.

TABLE 1 Weight contribution of early build-up phase (t = 0 to t_a) of $C_a(t)$, $C_O(t)$ and $C_H(t)$ on the calculated parameters T, C_2, and C_3 obtained from the late build-up phase (3 - 8 min). F = 50 ml/min/100 g.

	Phase (t = 0 to t_a)		
	0-60 sec	0-120 sec	0-180 sec
$C_a(t)$ on T	0.8	4.9	16.6
$C_O(t)$ on C2	1.2	6.4	19.8
$C_H(t)$ on C3	0.6	3.7	14.2

TABLE 2 % overestimation of CBF due to delay and dispersion of Ca(t)

	CBF ml/min/100 g	Build-up method 3-8 min	8-13min	13-18min	Conventional steady-state method
Delay 3 sec	30	4.5	3.9	4.2	3.3
	50	3.7	3.9	4.1	4.3
	80	5.9	5.4	5.1	6.0
Delay 5 sec	30	6.8	6.8	6.0	5.5
	50	6.9	7.1	7.1	7.4
	80	10.2	9.7	9.6	10.3
Delay 2.5 sec and dispersion 2.5 sec	30	6.8	6.0	6.3	5.5
	50	6.8	7.1	7.3	7.4
	80	10.1	9.6	9.3	10.3
Dispersion 5 sec	30	6.8	6.0	6.2	5.5
	50	6.8	7.0	7.2	7.3
	80	10.1	9.4	9.2	10.2

TABLE 3 Statistical noise of CBF images.

	ΔCBF/CBF	
CBF (ml/min/100 g)	Late build-up (3-8 min)	Near steady-state (8-13 min)
20	0.00054	0.00048
50	0.00089	0.00101
80	0.00106	0.00114

ΔCBF/CBF was calculated with the relationship

$$\Delta T = k\sqrt{T}$$

$$\frac{\Delta F}{F} = k\frac{EP(F)}{\sqrt{G^{-1}(F)}}$$

where F is CBF, EP(F) is the error propagation factor at F, and G is lookup table from tissue activity to flow. Constant k was omitted in the table.

TABLE 4

In vivo comparison of the calculated parameters for the new method with late build-up phase (3-8 min) and near steady-state phase (8-13 min) and the conventional steady-state method.

	Steady-state method	New method	
		(3-8 min)	(8-13 min)
CBF(ml/min/100g)	33.7 ± 12.3	36.6 ± 11.1 *	33.8 ± 11.5
OEF	0.455 ± 0.102	0.445 ± 0.077	0.440 ± 0.082
$CMRO_2$ (mlO_2/100ml/min)	2.68 ± 0.97	2.92 ± 0.80	2.69 ± 0.86

Values are mean ± SD (N = 8).

* $P < 0.01$ (ANOVA) for comparison with conventional steady-state method and near steady state phase of new method.

Figure Legends

FIGURE 1
Scan and reconstruction protocol for build-up method.

FIGURE 2

Mean arterial input functions of 8 patients in CBF study using $C^{15}O_2$ inhalation for $C_a(t)$ (A) and $^{15}O_2$ inhalation for $C_O(t)$ (B) and $C_H(t)$ (C). Each arterial input function was normalized with the mean value of steady state, that is, from 10 to 18 min. Mean $\pm$ SD was plotted at each time point of measurement.

FIGURE 3

Error propagation factors from measured tissue activity to CBF by the new method with early build-up phase (closed circles) and with near steady-state phase (open circles), and by the conventional steady-state method (open triangles). Error propagation factor is systematically smaller in the new method with early build-up phase (3-8 min) than in the conventional steady-state method, but in the steady-state phase (8-13 min), both methods show almost equivalent error propagation in the range of 20 to 100 ml/min/100 g.

FIGURE 4

Effect of flow heterogeneity on CBF measurement by the new method with early build-up phase (closed circles) and with near steady-state phase (open circles), and by the conventional steady-state method (open triangles). Error in measured flow was calculated for a ROI containing varying proportions of two tissues with different flows, that is, 80 ml/min/100g for gray matter and 20 ml/min/100 g for white matter. The partition coefficient was fixed to unity. Note that systematic underestimation of CBF is smaller in the late build-up phase than in the steady-state phase.

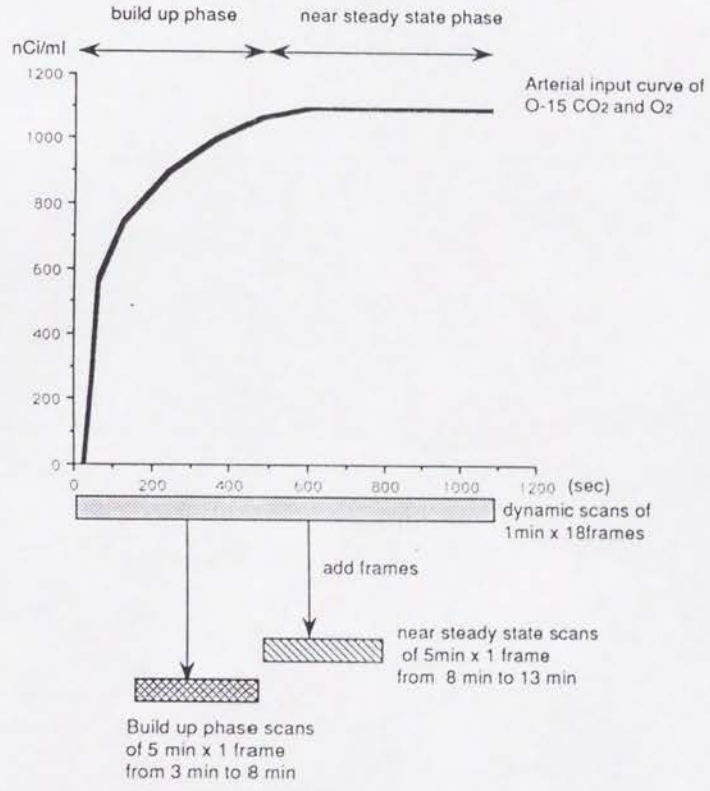
build up phase
near steady state phase
nCi/ml
1200
1000
800
600
400
200
0
Arterial input curve of
O-15 CO2 and O2
0
200
400
600
800
1000
1200
(sec)
dynamic scans of
1min x 18frames
add frames
near steady state scans
of 5min x 1 frame
from 8 min to 13 min
Build up phase scans
of 5 min x 1 frame
from 3 min to 8 min

Figure - 1

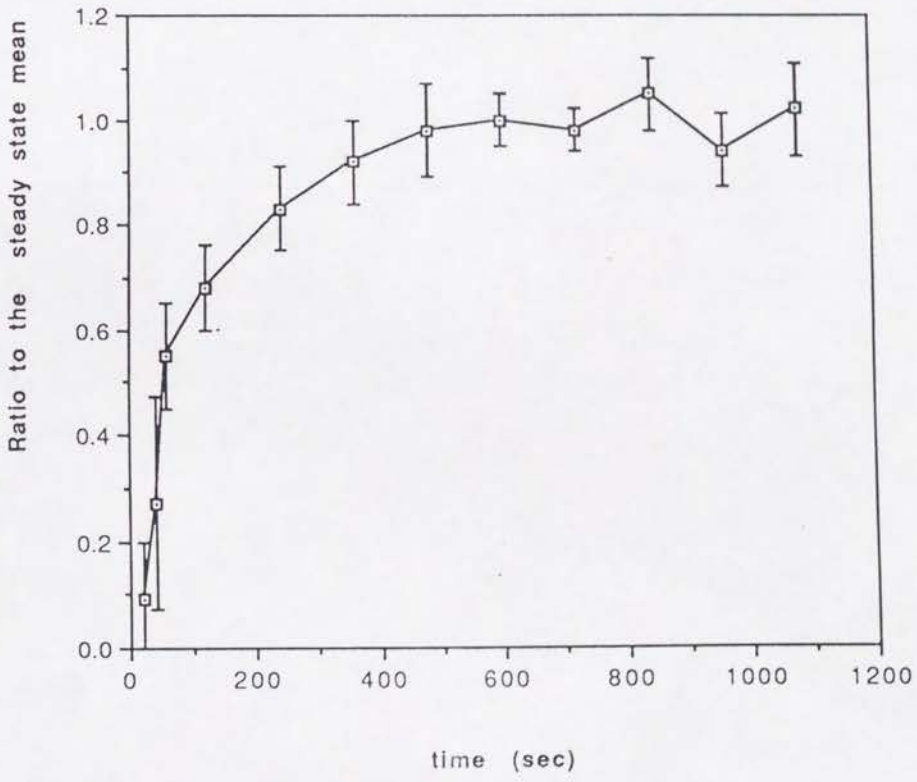
Ratio to the steady state mean
1.2
1.0
0.8
0.6
0.4
0.2
0.0
0
200
400
600
800
1000
1200
time (sec)

Figure 2A

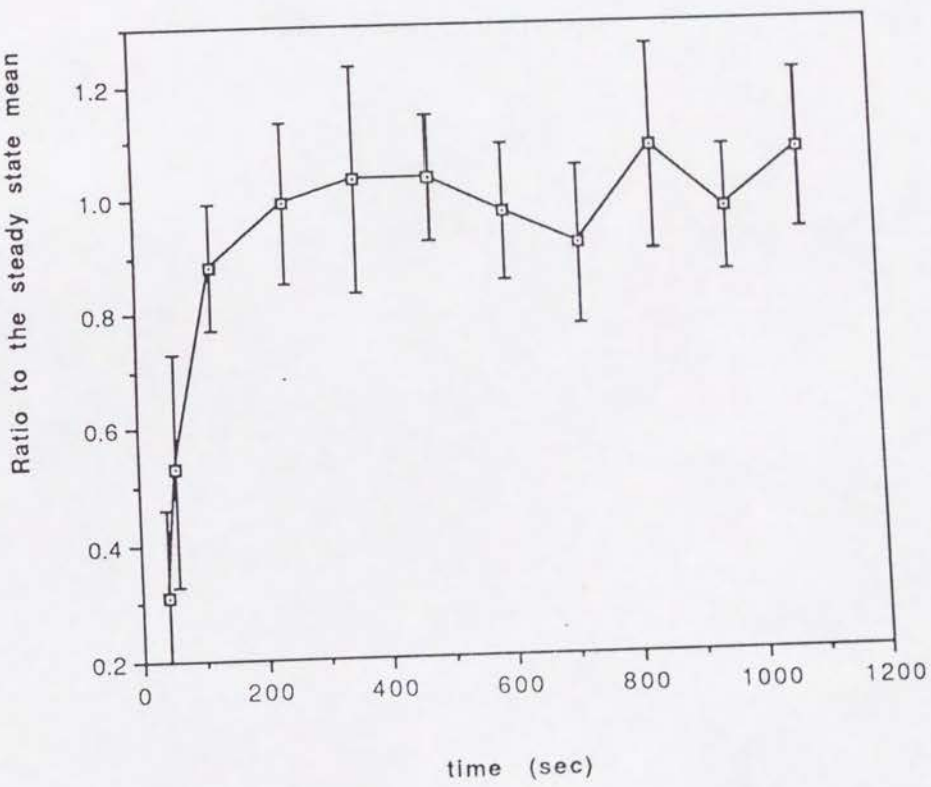
Ratio to the steady state mean
1.2
1.0
0.8
0.6
0.4
0.2
0
200
400
600
800
1000
1200
time (sec)

Figure 2B

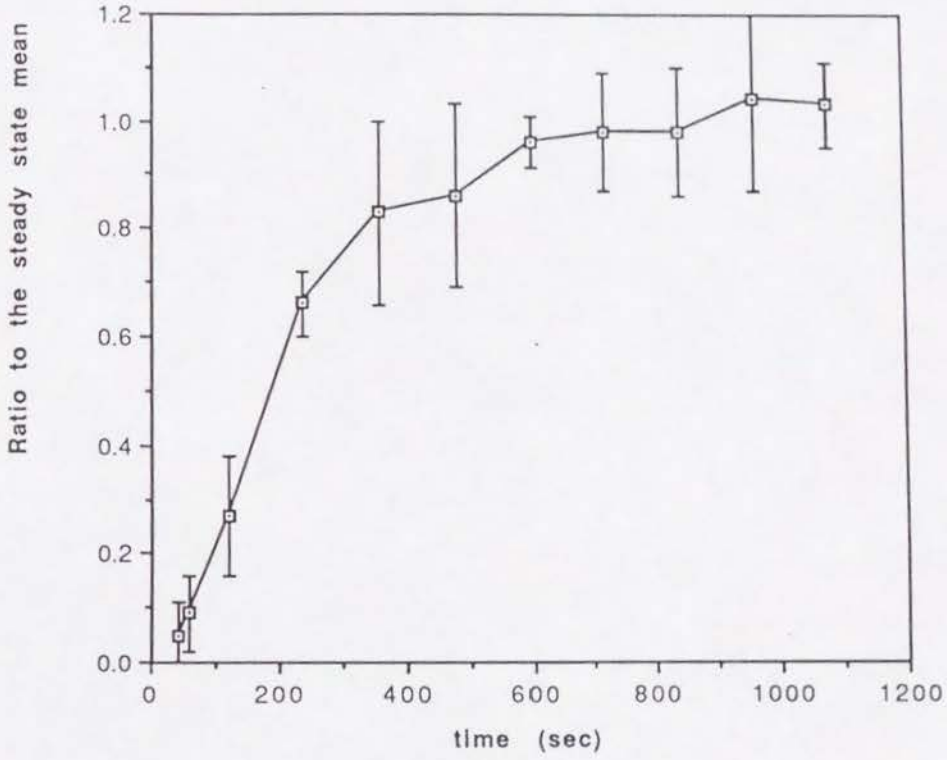
Ratio to the steady state mean
1.2
1.0
0.8
0.6
0.4
0.2
0.0
0
200
400
600
800
1000
1200
time (sec)

Figure 2C

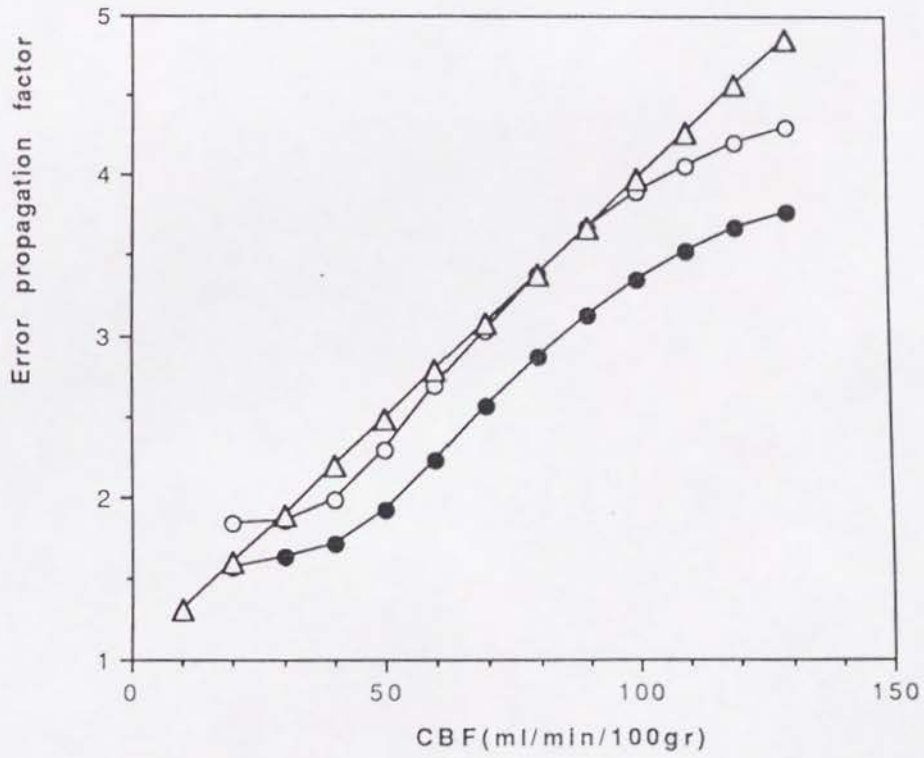

Figure 3

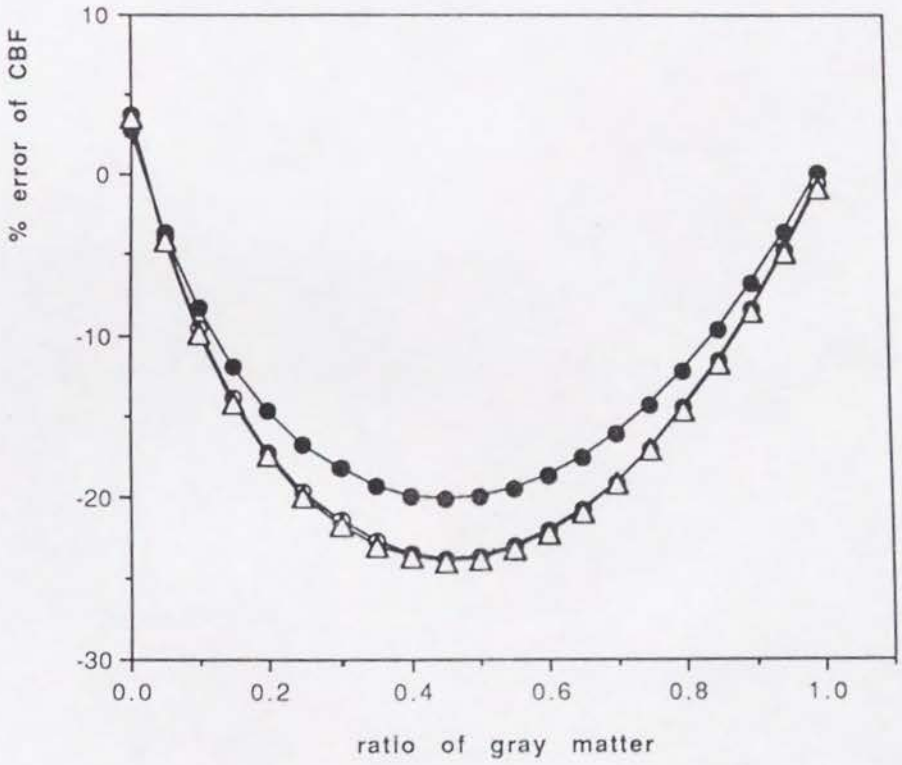

Figure 4